Clim Dyn (2017) 48:151–168
DOI 10.1007/s00382-016-3066-y

Intensity–area–duration analysis of droughts in China 1960–2013

Jianqing Zhai[1,3] · Jinlong Huang[2,4] · Buda Su[1,2,3,5] · Lige Cao[1,3] · Yanjun Wang[1] · Tong Jiang[1,3] · Thomas Fischer[3,6]

Received: 18 September 2015 / Accepted: 4 March 2016 / Published online: 18 March 2016

Abstract In this study, the intensity, area, and duration of droughts in China are analyzed using the Standardized Precipitation Index (SPI). The SPI was calculated on monthly data for 530 meteorological stations in China for the period 1960–2013. The time series were analyzed for ten major hydrological regions of China, respectively. The relationships between the intensity and the area of droughts for a specific duration were analyzed by the intensity–area–duration method. The results show that areas with a significant trend in dryness can be found in a band reaching from the southwest to the northeast of China, while areas with significant trends in wetness are especially detected in the northern river basins in recent decades. In addition, for recent years (2000–2013), most of the ten major hydrological regions show opposite trends in the SPI when compared to the whole study period (1960–2013) except for the central and southwestern parts of China. This dryness/wetness trends are related to the intensity and duration of drought events, which have been stronger and lasted longer in the detected dryness band except for some northern river basins. A regional shift of drought centers is found from the northwest to the southeast within Central China. Moreover, a decreasing trend in drought area is observed, which might be related to the regional changes in precipitation pattern associated with the atmosphere–ocean interaction. Changes in the SST of the Tropical Pacific and the Tropical Indian Ocean may have resulted in frequent severe drought events of small areal extent in the central and southwestern parts of China. For the study period, the most severe droughts that covered large areas mainly occurred in the north and west of China during the mid-to-late twentieth century. However, in the early twenty-first century, the most severe droughts were located in the southwest of China covering areas less than 0.7 million km^2. Conclusively, drought areas show a decreasing tendency, while more intense droughts of longer duration have been experienced, especially in the south of China, in the last decades.

Keywords Drought · Intensity · Area · Duration · China

✉ Buda Su
subd@cma.gov.cn

✉ Thomas Fischer
tom.fischer8@gmx.de; thomas.fischer.geo@gmx.de

[1] Collaborative Innovation Center on Forecast and Evaluation of Meteorological Disasters/School of Remote Sensing, NUIST, Nanjing 210044, China

[2] State Key Laboratory of Desert and Oasis Ecology, Xinjiang Institute of Ecology and Geography, Chinese Academy of Sciences, Urumqi 830011, China

[3] National Climate Center, CMA, Beijing 100081, China

[4] University of Chinese Academy of Sciences, Beijing 100049, China

[5] Potsdam Institute for Climate Impact Research, Potsdam, Germany

[6] Department of Geosciences, Eberhard Karls University, Tübingen, Germany

1 Introduction

Almost all parts of the world are experiencing a warming trend since the late twentieth century (Hansen et al. 2010; Lawrimore et al. 2011; Rohde et al. 2013). Influenced by the changing climate, the intensity, extent and duration of extreme events (e.g. drought) can result in an unprecedented severity (Field et al. 2012). Drought is one of the most widespread nature hazard has profound effects on ecosystems, hydrology, agriculture, and the economy (Vicente-Serrano

et al. 2012; Narasimhan and Srinivasan 2005). Understanding the spatial and temporal characteristics of drought is important for mitigating the impacts of drought and managing the drought risk (Mishra and Singh 2010; He et al. 2011).

Drought as a spatial–temporal process is usually characterized by its intensity, spatial extent, and duration at a regional scale (Xu et al. 2015; Sheffield and Wood 2007; Sheffield et al. 2009). In previous studies, drought was usually analyzed using one-dimensional methods without considering the spatial extent (Bordi et al. 2005; Kamali et al. 2015; Smerdon et al. 2014). There, the intensity, peak values, and duration of droughts are extracted from time series for a fixed area (e.g. station or basin) (Biondi et al. 2008).The severity–area–duration (SAD) method proposed by Andreadis et al. (2005) provides a new perspective to analyze drought in a space–time dimension. SAD curves have been built for different regions showing the intensity of droughts in relation to the area at different durations (Andreadis et al. 2005; Sheffield et al. 2009; Samaniego et al. 2013; Kyoung et al. 2011).

Almost all regions in China are prone to drought. Here, the drought-affected crop area averages 209,000 km^2 per year for the period from 1949 to 2013, which is equivalent to 1/6 of the total arable land. Annual direct economic losses reach more than 32 billion Yuan according to 2013 price levels (Qin et al. 2015; Zhai et al. 2014). Therefore, the analysis of such droughts is an essential part in the reduction of drought impacts in China. In several studies, droughts in China were analyzed regionally by using drought indices based on observed meteorological data. For example, droughts in the Yellow River basin occurred frequently during the period of 1960–2009 (Qian et al. 2011). Significant trends toward dry conditions were detected in the northeastern river basins, the middle part of the Yangtze River basin, and the Southwest of China, while significant changes toward wet conditions were found in the northwestern parts of China and the upstream and lower reaches of the Yangtze River basin (Shi et al. 2003; Zhai et al. 2010; Zhao et al. 2012; Tao et al. 2014). In recent years, more frequent and severe droughts occurred in the northeastern parts of China (Yu et al. 2014). In the Huaihe River basin, drought events occurred more frequently since the 1980s (Yang et al. 2012a). The frequency of extreme droughts also significantly increased in Southwest China during the period 1960–2009, and especially in the 2000s (Zhang et al. 2013a). Significant dry periods became longer from 1961 to 2007 in the Zhujiang River basin (Fischer et al. 2011). Droughts in China occurred more frequently and severely in recent decades than in previous decades mainly in regions from southwest to northeast of China.

Few studies exist that focus on drought analyses for China at space–time dimensions. Based on five adjacent stations experiencing drought conditions, regional drought events are analyzed by Qian et al. (2011) on their spatial extent. In order to better understand the regional drought characteristics in China, this current study focuses on the changes in drought intensity, drought areal extent, and drought duration, and the relationship among these in a space–time dimension by relating the intensity and area of drought at predefined durations similar to the SAD method based on the Standardized Precipitation Index (SPI) for the period 1960–2013. The data and method used in the study are described in the next section. The results of the trend analysis in the SPI of the ten major hydrological regions, the analysis of drought characteristics, and their space–time-relationships are presented in Sects. 3, 4, and 5, respectively.

2 Data and methodology

2.1 Study area and datasets

For this analysis, China is subdivided into ten hydrological regions, i.e. the Songhuajiang River basin, the Liaohe River basin, the Haihe River basin, the Yellow River basin, the Huaihe River basin, the Yangtze River basin, the Zhujiang River basin, the Southeast river basins, the Southwest river basins, and the Northwest river basins (the latter three regions consist of several small river basins) (Fig. 1). China has a complex topography with mountain ridges, river basins, plateaus, hills, and plains. The average annual precipitation decreases from the Southeast to the Northwest of China. Regions with an annual precipitation exceeding 800 mm are regarded as humid regions, 400–800 mm as semi-humid regions, 200–400 mm as semi-arid regions, less than 200 mm as arid regions (Fig. 1).

Monthly precipitation datasets from 752 meteorological stations in China for the period 1960–2013 were provided by the National Meteorological Information Center of the China Meteorological Administration. Among those, 530 stations were chosen for further calculations based on strict selection criteria including data quality, continuity, homogeneity, and the length of the records.

2.2 Drought index

For the comparison of regions with different climate and soil characteristics, the dryness or wetness conditions can be characterized by various drought indexes. The SPI is one of the most applied drought indices, and is calculated using long-term records of monthly precipitation time series with at least 30-year records (Wu et al. 2005). The SPI is developed by fitting the monthly precipitation to a Gamma distribution, which is then transformed to a normal distribution with the mean of zero and variance of one (McKee et al. 1993). This normally standardized index allows the

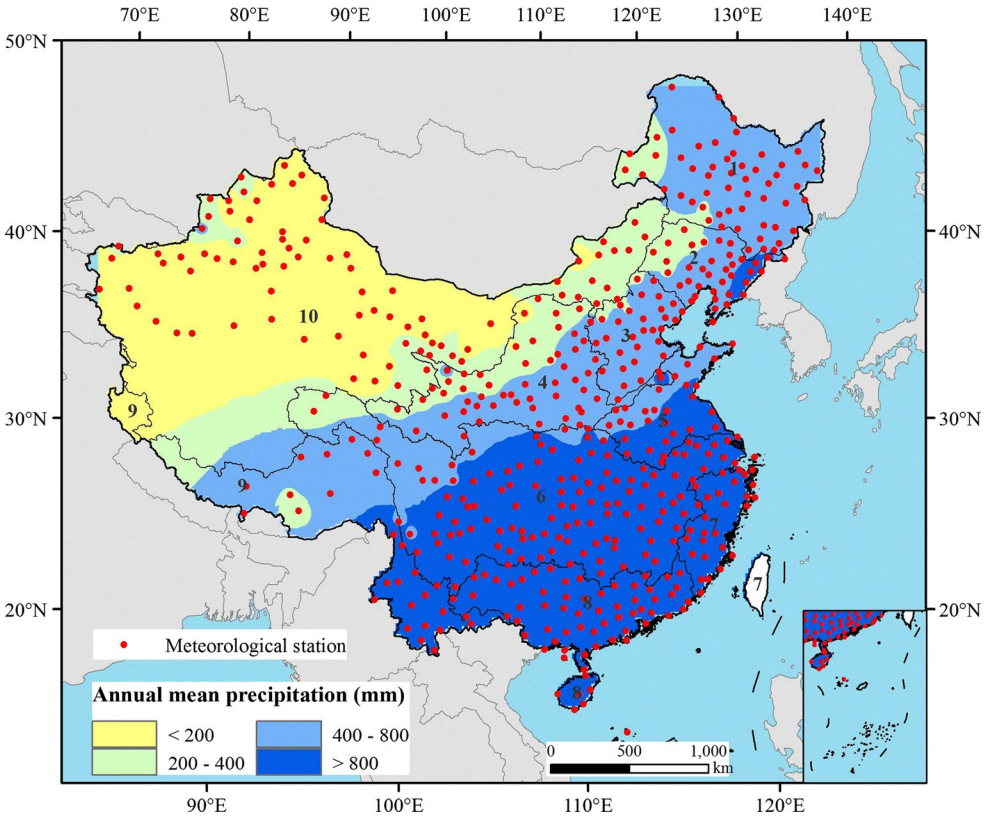

Fig. 1 Location of 530 meteorological stations and the ten major hydrological regions in China analyzed in this study (1 = Songhuajiang River basin; 2 = Liaohe River basin; 3 = Haihe River basin; 4 = Yellow River basin; 5 = Huaihe River basin; 6 = Yangtze River basin; 7 = Southeast river basins; 8 = Zhujiang River basin; 9 = Southwest river basins; 10 = Northwest river basins)

Table 1 Classification of dry or wet conditions of the SPI

SPI	Categories
≥2.0	Extremely wet
1.5 to 1.99	Severely wet
1.0 to 1.49	Moderately wet
−0.99 to 0.99	Near normal
−1.49 to −1.0	Moderately dry
−1.99 to −1.5	Severely dry
≤− 2.0	Extremely dry

comparison of all stations in the study area with the same thresholds used to identify significant dry or wet conditions (Table 1). The SPI can be calculated at multiple time scales such as 1-, 3-, 12-month. The various different scales are explained by the preprocessing of the precipitation time series. For the *i*-month time scale, a window length of *i* months has been used to accumulate the precipitation. This precipitation preprocessing is defined as:

$$Result_{k+i-1} = \sum_{k=1}^{n-i+1} P_k$$

where *i* denotes the time scale, P_k is the monthly precipitation at *k* time, and *n* is the length of the precipitation record for the station.

In general, the 1 to 3-month SPI is strongly affected by monthly moisture changes, and is therefore used to reflect the status of soil moisture. The changes in soil moisture in the lower layers as well as in river runoff are better reflected with a 6 to 24-month SPI. Hence, the 12-month SPI is used in this study to analyze the characteristics of hydrological drought (WMO 2012) in China. This is further supported by the high correlation coefficients between the annual averaged 12-month SPI and the runoff anomaly found for numerous river basins in China (Zhai et al. 2010).

2.3 Trend analysis

The variation and its significance in the SPI time series are tested by the non-parametric Mann–Kendall test, which is widely used in climatology and hydrology (Tao et al. 2011). For a time series with a size of *n*, the processes of the Mann–Kendall test method are described as follows. Firstly, the statistical parameter s_k is calculated as:

$$s_k = \sum_{i=1}^{k} r_i \quad (k = 2, 3, \ldots, n)$$

$$r_i = \begin{cases} +1 & if\ P_i > P_j \\ 0 & if\ P_i = P_j \\ -1 & if\ P_i < P_j \end{cases}$$

where P_i denotes the precipitation at time i. The variance of s_k is then defined as:

$$\mathrm{Var}(s_k) = \frac{n(n-1)(2n+5)}{18}$$

The MK statistic is defined as:

$$MK_k = \begin{cases} \frac{[s_k-1]}{\sqrt{\mathrm{Var}(s_k)}} & if\ s_k > 0 \\ 0 & if\ s_k = 0 \\ \frac{[s_k+1]}{\sqrt{\mathrm{Var}(s_k)}} & if\ s_k > 0 \end{cases}$$

When $|MK_k| > 1.96$, the trend of the time series is significant at the 95 % confidence level. $MK_k > 1.96$ means a significant increase, $MK_k < -1.96$ denotes a significant decrease. In this study, time series with MK-values below the 95 % confidence level are only considered as tendencies.

2.4 Intensity–area–duration analysis

A drought event can be defined as a process of continuous dry conditions for a specific duration (from the formation to the end) and over a contiguous area. For each time step (month), the extent of droughts can be identified by the cluster analysis method as described in Andreadis et al. (2005) and Sheffield et al. (2009). For this, the monthly precipitation is interpolated to a grid field with a resolution of 0.5° × 0.5° covering whole China by applying the inverse distance weighting (IDW) method described by Gemmer et al. (2004). Afterwards, for each grid (i.e. square) the 12-month SPI is calculated. In the following, the grids with an SPI below −1 (moderate drought or more severe) are identified and assigned to the drought category. Starting from the grid with the lowest SPI value (i.e. highest drought intensity), the adjacent grids (3-by-3 neighborhood grids) are checked if they belong to the drought category. The procedure is repeated until no grids are in the neighborhood of the current cluster of grids belonging to the drought category. If grids of the drought category exist outside of the current cluster, a new cluster is created using the same procedure as above. At the end, separate drought clusters with different contiguous area sizes are identified for one time step (i.e. 1 month). The drought intensity of each cluster is defined as the mean SPI value of all grids within the cluster. The contiguous drought area is obtained by the sum of all grids' area, which is measured by using the spatial area tool of ArcGIS 10.

When generating the IAD curves, the drought duration is predefined for 1, 3, 6, 9, 12, and 24 months. Drought with duration t is firstly identified (SPI < −1) at each grid for each time step (time step i represents the time interval from time i to $i + t - 1$). The drought intensity (I) is then defined as $I = \sum SPI/t$, where $\sum SPI$ is the SPI summed over duration t for each grid. For each time step i, the IAD analysis is based on the cluster algorithm, which starts at the grid containing the lowest SPI value (drought center). By attaching the adjacent grids with low SPI values within the drought category, the area and the intensity is calculated and recorded based on the summed area of grids and the average intensity until the maximum spatial extent of the drought event is reached. For each cluster (i.e. drought event), an IAD curve can be generated using the records described above at the specific duration t (Fig. 2a–f). In this paper, these IAD curves are calculated for the predefined duration of 1, 3, 6, 9, 12, and 24 months, respectively. The highest intensity at a contiguous drought area for a specific duration is presented by the IAD envelope curve (Fig. 2g). While the IAD curve can be used to compare drought events on different intensity and area, the IAD envelope curve identifies the highest intensity at each contiguous drought area for the whole study period.

3 Statistical trend analyses of SPI time series

The spatial patterns of trends in the SPI index at meteorological stations in China are displayed in Fig. 3a. The positive or negative tendencies and significant trends in the SPI are calculated based on the MK statistics (Table 2) for the observed period from 1960 to 2013. Statistically significant negative trends towards more dry conditions are found in many stations located in the Songhuajiang River basin (30 % of all stations in the river basin), Liaohe River basin (46 %), Haihe River basin (63 %), Yellow River basin (55 %), in the middle part of the Yangtze River basin (31 %), the western part of the Zhujiang River basin (30 %), and the southeastern part of the Southwest river basins (35 %). All these stations with a significant negative trend are located in a belt from the southwest to the northeast of China. In contrast, many stations in the northwestern mountainous part of the Northwest river basins (78 % of all stations in the river basin), the upper and lower parts of the Yangtze River basin, the northern part of the Southwest river basins (31 %), and the Southeast river basins (68 %) show significant positive trends, i.e. a trend towards more wet conditions (Fig. 3a; Table 1).

As for the more current short-term period from 2000 to 2013 (Fig. 3b), significant increases in the SPI are detected in the northern river basins (of the Songhuajiang, Liaohe, Haihe, and Yellow Rivers) and a significant decrease in the Northwestern river basins, which is in contrast to the long-term trends. This indicates that the arid and semi-arid region experienced more diverse dry and wet conditions during the last one-and-a-half decades, as the long-term trend would suggest. Noticeable are the relatively stable trends in the southern more humid areas for both analyzed trend periods.

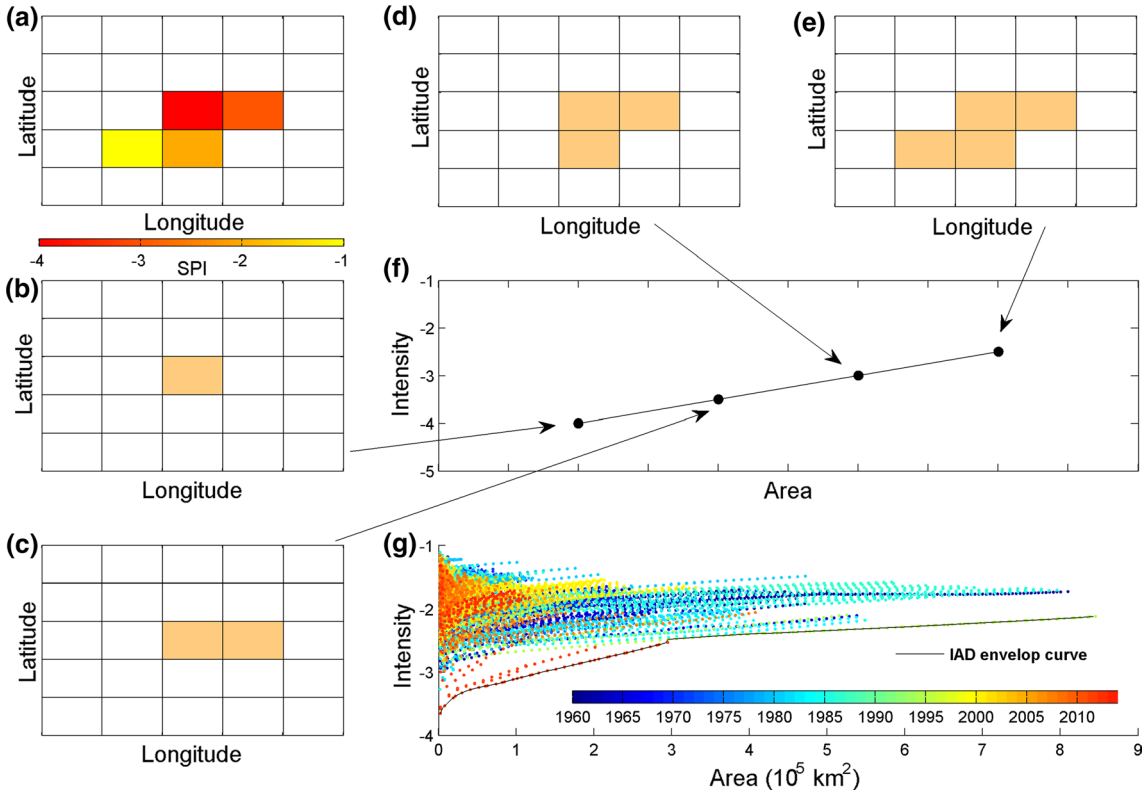

Fig. 2 Construction of the IAD curve and IAD envelop curve

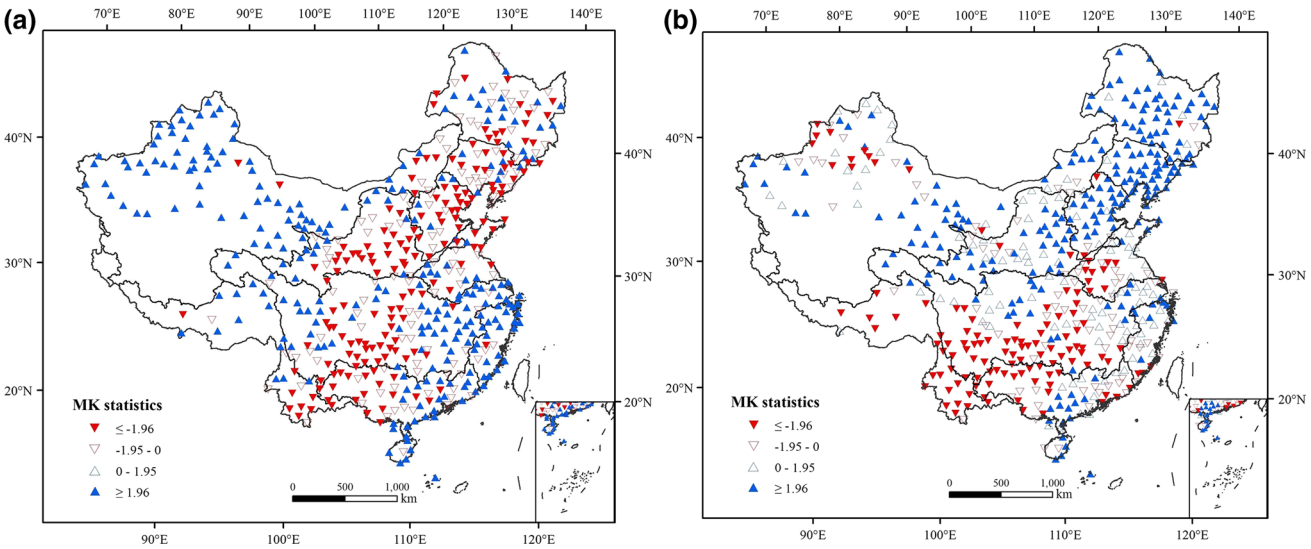

Fig. 3 Spatial distributions of tendencies or trends in the SPI-12 at meteorological stations in China for the period **a** 1960–2013 and **b** 2000–2013; the *inverted red filled triangle* indicates a significant decreasing trend, while the *blue filled triangle* indicates a significant increasing trend

The Basin-averaged SPI is calculated and tested by the Mann–Kendall non-parametric method. As shown in Table 2, significant trends toward dryer conditions (negative MK statistic) are averagely found in the Liaohe River basin, Haihe River basin, Yellow River basin, and the Huaihe River basin. Trends toward wetter conditions are found in the Southeast river basins and the Northwest river basins. All the other hydrological regions show

Table 2 Trend statistics and proportion of meteorological stations with significant trend in the ten hydrological regions of China for the period 1960–2013

Trend	Region									
	Songhuajiang	Liaohe	Haihe	Yellow River	Huaihe	Yangtze River	Zhujiang	SE river basins	SW river basins	NW river basins
Significant increase (%)	17	3	3	11	16	30	27	68	31	78
Significant decrease (%)	30	46	63	55	33	31	30	4	35	8
Mann–Kendall statistics	−1.42	−3.53*	−4.68*	−4.25*	−2.07*	−1.05	−0.59	5.34*	−1.20	12.65*

* Significant at the 95 % confidence level

rather tendencies toward dryer conditions without passing the 95 % confidence level. For the decadal changes in the SPI time series, all northern river basins (Songhuajiang, Liaohe, Haihe, Yellow, and Huaihe River basin), except the Northwest river basins, show a cyclical 'dryness-wetness' pattern, with a tendency towards dryness before the twenty-first century and a wetness tendency in the beginning of the twenty-first century, while the Northwest river basins experience a rather persistent wetness trend. In contrary, the southern river basins (Yangtze, Zhujiang, Southwest, and Southeast river basins), show contrasting and only small cyclical 'wetness–dryness' patterns, with a wetness tendency before the twenty-first century and a tendency towards dryness in the beginning of the twenty-first century (Fig. 4). At river basin scale, no definite historical trends but more or less distinct oscillations in the SPI time series are obvious for most river basins, except the Northwest and Southeast river basins, which show rather persisting long term trends toward dryness. The western and northeastern river basins experienced stronger magnitudes in the SPI in the early twenty-first century supporting the assumption of intensification due to global warming. The other river basins experienced rather stable magnitudes implying a typical oscillation without intensification due to global warming.

4 Drought characteristics

4.1 Frequencies of drought

The regional variations in drought conditions, e.g. number of total droughts and average drought duration, are shown in Fig. 5. Small numbers of drought events are mainly found in the arid and semi-arid regions, while most drought events (more than 22 events during 1960–2013) occur in humid regions (Fig. 5a). The number of drought events is calculated without considering their individual duration. As shown in Fig. 5b, the arid and semi-arid regions show higher average drought durations, while shorter average drought durations are located in the humid regions. The total number of months with drought is equivalent to the number of drought events multiplied by the average drought duration. The spatial distribution of drought events with certain durations (months) is shown in Fig. 5c-f. Short-term drought events (1–3 months) occur most often in the middle and lower Yangtze River basin, the middle of the Zhujiang River basin, and in the Southeast river basins with over 14 drought events observed in 1960–2013. The highest frequencies of short-to-medium-term drought events (4–6 months) are similarly distributed as for the short-term drought events but with up to 9 drought events. Medium-term drought events (7–12 months) occur most frequently in a band from the southwest (upper southwest river basins) to the northeast (middle of the Songhuajiang River basin) of China. The most long-term drought events (>12 months) have been observed in the north of the Northwest river basins as well as in the southeast river basins with 3 to 4 drought events. It can be seen that short-term drought events occur more often in humid regions, while long-term drought events are more common in arid and semi-arid regions of China.

4.2 Changes in drought intensity and duration

Based on the SPI, the drought events are analyzed on their trends in intensity and duration. The intensity is calculated by the averaged SPI over the duration of a drought event (SPI < −1) for each station and tested on significance by the Mann–Kendall test. The spatial distribution of the trends and tendencies in drought intensity for the period of 1960–2013 is shown in Fig. 6a. Increasing trends in drought intensity are mainly located in the Songhuajiang River basin, Liaohe River basin, the middle of the Yellow and Yangtze River basins, the southeast of the Southwest river basins, the western part of the Zhujiang River basin, and in the Southeast river basins. Decreasing trends in drought intensity are mainly found in the northwestern mountainous part of the Northwest river basins, the north of the Southwest river basins, the upper and lower Yangtze River basin, the HaiheRiver basin and in the eastern part of the Zhujiang River basin.

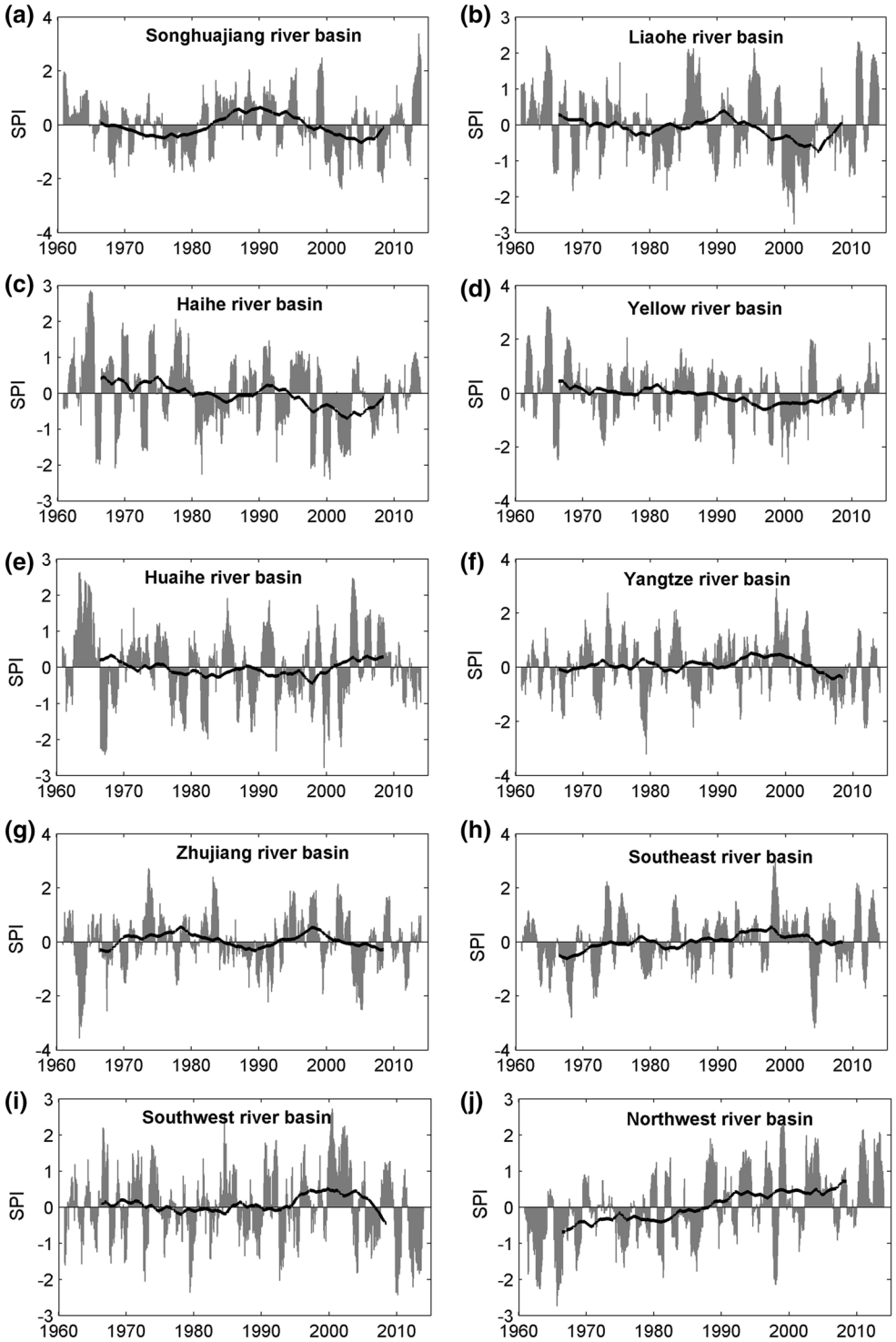

Fig. 4 Average SPI-12 time-series of the ten major hydrological regions of China for 1960–2013 (**a** Songhuajiang River basin, **b** Liaohe River basin, **c** Haihe River basin, **d** Yellow River basin, **e** Huaihe River basin, **f** Yangtze River basin, **g** Zhujiang River basin, **h** Southeast river basins, **i** Southwest river basins, **j** Northwest river basins); the *dark line* shows the 10-year moving average

Similar to the intensity, the changes in the duration of drought events at each meteorological station are presented in Fig. 6b. The spatial patterns are very similar to that of drought intensity, hence, the spatial correlation coefficient between the MK statistics of intensity and duration is significant at around 0.61.

4.3 Changes in drought area

Changes in the total area affected by drought, the average contiguous drought area, and in the maximum contiguous drought area for a specific duration (1, 3, 6, 9, 12, and 24 months) are calculated based on the cluster analysis for each time step (i.e.

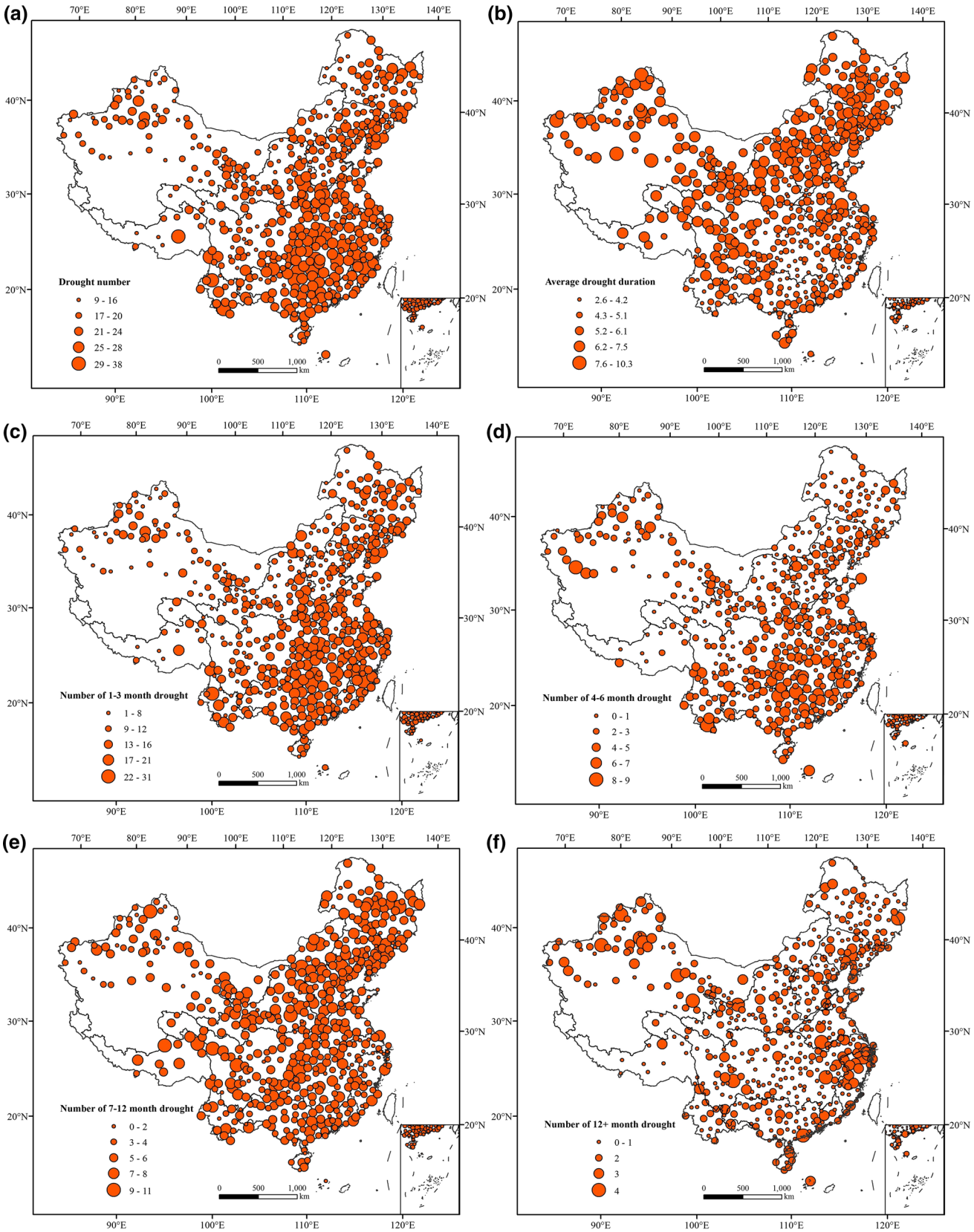
(a)
Drought number
9 - 16
17 - 20
21 - 24
25 - 28
29 - 38
(b)
Average drought duration
2.6 - 4.2
4.3 - 5.1
5.2 - 6.1
6.2 - 7.5
7.6 - 10.3
(c)
Number of 1-3 month drought
1 - 8
9 - 12
13 - 16
17 - 21
22 - 31
(d)
Number of 4-6 month drought
0 - 1
2 - 3
4 - 5
6 - 7
8 - 9
(e)
Number of 7-12 month drought
0 - 2
3 - 4
5 - 6
7 - 8
9 - 11
(f)
Number of 12+ month drought
0 - 1
2
3
4
0 500 1,000 km
70°E 80°E 90°E 100°E 110°E 120°E 130°E 140°E
40°N 30°N 20°N

◀**Fig. 5** Spatial distribution of drought characteristics over China for 1960–2013. **a** Number of drought events, **b** average drought duration, **c** number of short-term drought events (1–3 months), **d** number of short-to-medium-term drought events (4–6 months), **e** number of medium-term drought events (7–12 months), **f** number of long-term drought events (>12 months); months represent the duration of the drought event and the *number* denote how frequency the drought with predefined duration is at each meteorological station

each month starting from January 1960 until December 2013). The area of a contiguous drought event is calculated by the sum of the grids' areas with an SPI below −1 encompassed by this drought event and by definition larger than 50,000 km^2. The duration of a contiguous drought area is given, for example, with duration of e.g. 3 months, which started in September 1980 and lasted until November 1980. In the following, the drought areas are analyzed for different durations of 1, 3, 6, 9, and 12 months separately (Fig. 7).

The total area affected by droughts decreased significantly during 1960–2013. A decreasing trend was also detected in the average contiguous area of drought, with significant changes for drought events with duration of 1- and 3-month. Average contiguous areas of droughts with longer duration show no significant trends but decreasing tendencies for the period 1960–2013. The maximum contiguous areas of droughts, which represent the main drought affected areas in China, show a significant decreasing trend for 1-, 3-, 6-, 9-, and 12-month duration. Only for drought events with duration of 24 months, a weak increasing tendency can be found in the total area affected by drought, the average contiguous drought area, and the maximum contiguous drought area. The largest areas affected by droughts have been observed in the mid- and late-1980s.

To identify the spatial changes in drought area, the drought center (i.e. location of the lowest SPI) is extracted from the average contiguous drought area for each time step. The average location is in central China. During the period 1960–2013, a significant shift of the location of the drought center is found from the northwestern part of Central China towards the southeastern part of Central China. The decadal changes in the location of the drought centers are shown in Fig. 8. The variation in the longitude and latitude of the drought center for different durations clearly shows a shift from the northwest to the southeast. Based on the drought countrywide grid, the centers of all drought events with a contiguous area larger than 50,000 km^2 for different drought durations (1, 3, 6, 9, 12, and 24 months) are shown in Fig. 9. From the spatio-temporal patterns of the drought centers, especially for the long-term droughts, it is found that in the early decades of the study period, droughts occurred more frequently in the northwestern and northern regions of China, while for the late twentieth and early twenty-first century, most drought centers were located in a band from the northeast to the southwest of China.

5 Intensity–area–duration analyses

5.1 Comparison of drought events

Drought events are spatially analyzed at meteorological station level or river basin scale without considering the contiguous drought area. IAD curves provide a new perspective

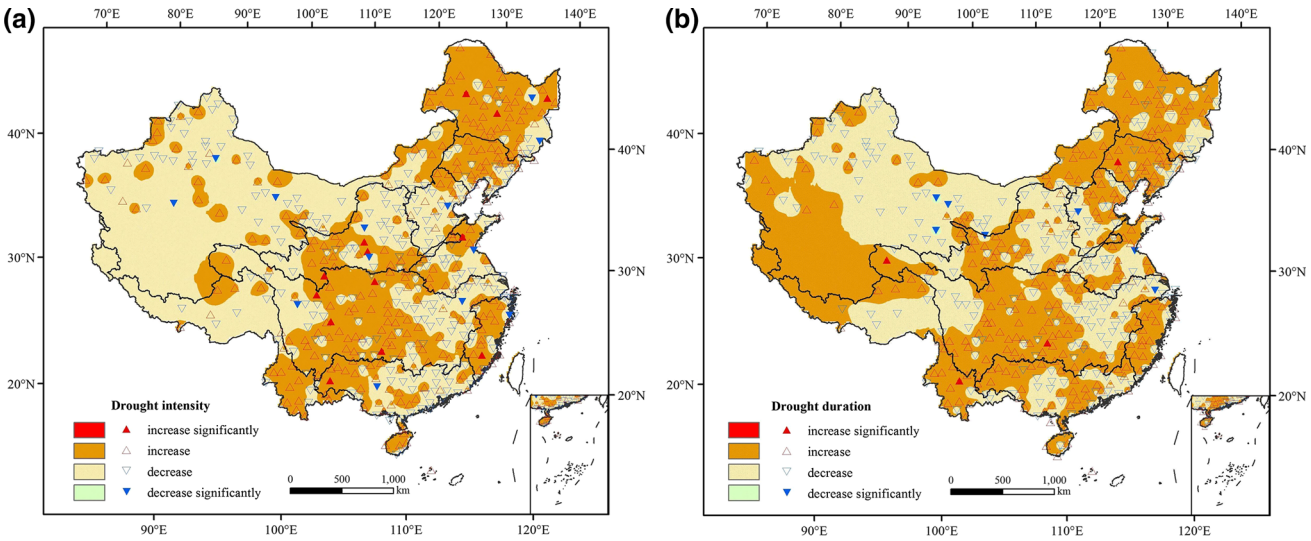

Fig. 6 Spatial distribution of tendencies or trends in **a** drought intensity and **b** drought duration at meteorological stations in China for the period 1960–2013; the *filled triangles* indicate significance at the 95 % confidence level; the *shadings* and *hollow triangles* show non-significant tendencies in drought intensity

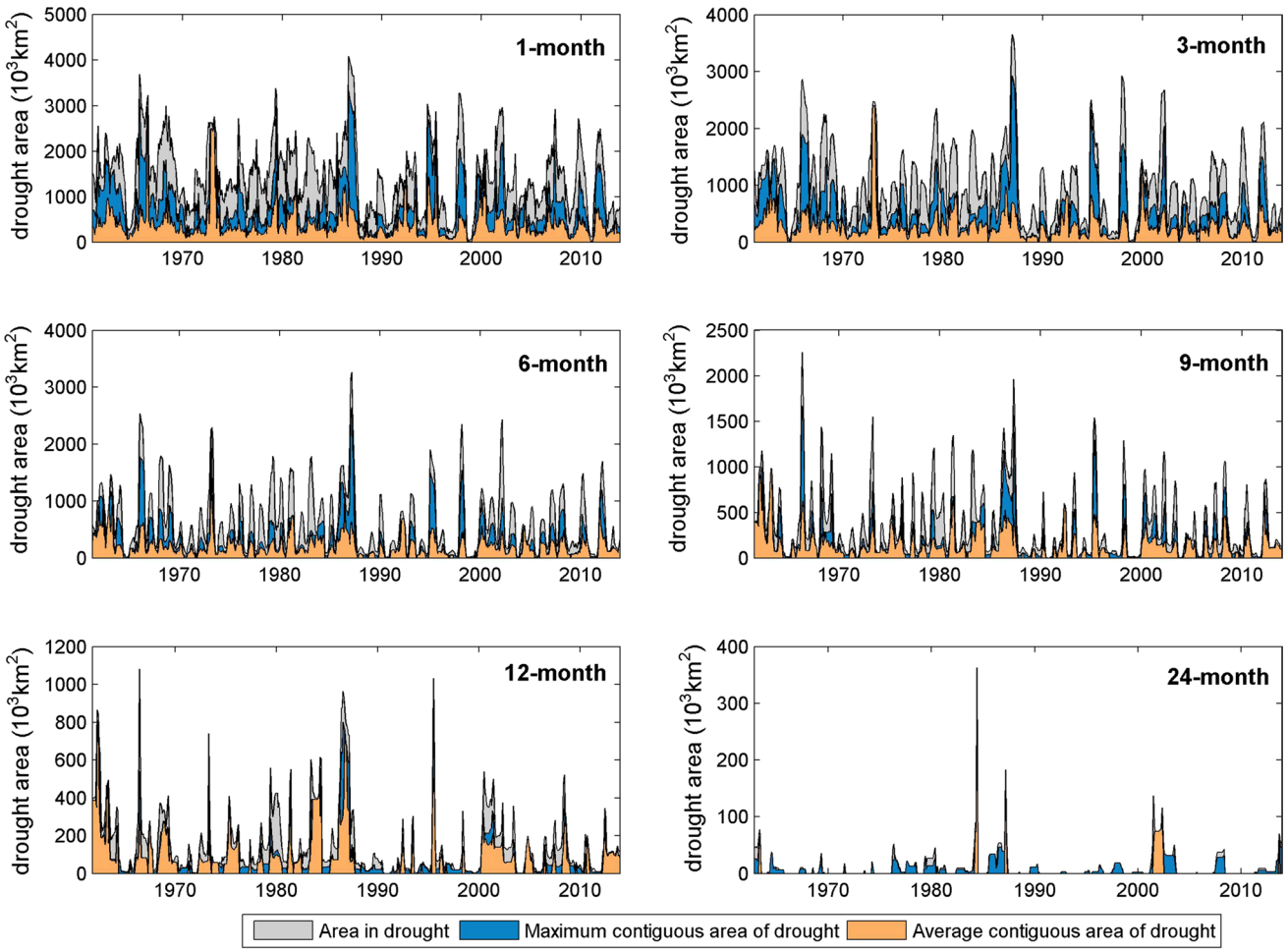

Fig. 7 Monthly time series of the total area affected by drought, the average contiguous drought area, and the maximum contiguous drought area for different durations (1-, 3-, 6-, 9-, 12-, 24-months) during the period 1960–2013; Area is calculated by the drought events that regard each time step as the starting month

to compare the drought events by considering the intensity, duration, and contiguous area of these droughts. Based on the monthly averaged region-wide SPI for whole China, the time-series of wet and dry conditions is visualized in Fig. 10f without considering the regions. Large negative peaks (below −1) indicate months with drought conditions. Five major drought events (SPI < −1) have been detected based on their average duration and intensity. As can be seen in Fig. 10f, the five major drought periods occurred (a) from May 1963 until December 1963, (b) from December 1978 until June 1979, (c) from September 1986 until April 1987, (d) from August 2004 until May 2005, and (e) from July 2011 until March 2012.

For the five major drought periods, the regional extents are shown in Fig. 10a–e. From May 1963 until December 1963, the droughts with 8-month duration were mainly found in the Zhujiang River basin. Severe droughts with 7-month duration from December 1978 to June 1979 were mainly located in the lower Yangtze River basin. Droughts with 8-month duration from September 1986 to April 1987 occurred in a bend along 30°N latitude. A rather small drought event with 10-month duration was found in the Songhuajiang River basin from August 2004 to May 2005. Droughts with 9-month duration from July 2011 to March 2012 occurred in Southwest China. In Fig. 11, the IAD curves for the detailed comparison of the five drought periods in China at regional scale are constructed for the durations of 1, 3, 6 and 9 months. Regarding the intensity, the drought from July 2011 until March 2012 is the most severe among the five drought events as it shows the lowest SPI values. The same drought covered a contiguous area of up to 0.7 million km^2 for its 9-month duration. The drought from September 1986 until April 1987 shows the largest contiguous area (more than 2 million km^2), which is illustrated by the longest curve. Among the five drought periods in China (during 1960–2013), the least severe event with additionally the smallest affected area happened from August 2004 until May 2005, but was still lasting more than 9 months.

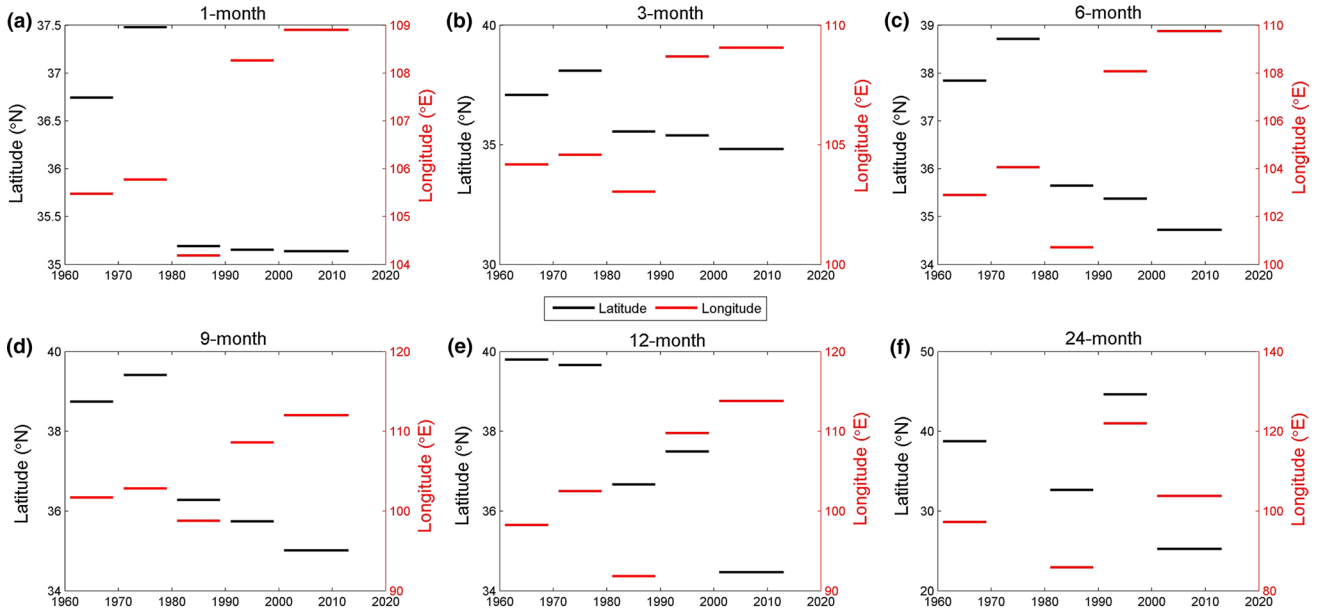

Fig. 8 Decadal changes in the location (latitude/longitude) of drought centers of all droughts with a contiguous area above 50,000 km^2 for different durations (1-, 3-, 6-, 9-, 12-, 24-months) in China for 1960–2013

5.2 The IAD envelope curves

To identify the most severe drought events of the entire period (1960–2013) with considering the regional area, the IAD envelope curves for different durations are visualized and interpreted (Fig. 12a). IAD envelope curve provides the time of occurrence and intensity of a regional drought with a contiguous area larger than 50,000 km^2 at a predefined duration (1, 3, 6, 9, 12, and 24 months). The IAD envelope curves as shown in Fig. 12a, depict five main drought periods (1965–1966, 1982–1984, 1986–1987, 1994–1995 and 2011–2012) during the study-period. Two drought periods (1986–1987 and 2011–2012) are similar to the results of the IAD analysis of five selected drought period mentioned in Sect. 5.1, all others show higher individual values for the investigated durations.

In addition to the IAD envelope curves, the spatial locations of the centers of these events are shown in Fig. 12b. The most recent drought (2011–2012), which occurred in the southwest of China, was the most severe drought events with a duration from 3 to 9 months at a relatively small contiguous area under 0.7 million km^2. For the slightly larger contiguous area between 0.7 and 1.1 million km^2, the drought of 1994–1995 was the most intensive. This drought period also had the highest intensities for the 1- and 3-month durations with larger spatial extents (more than 2 million km^2). For the contiguous areas from 1.1 to 1.8 million km^2, the most intensive drought events with a duration from 3 to 9 months occurred in the north of China in 1965–1966. The largest contiguous area under drought with the highest intensity for the durations from 1 to 6 months was observed in 1986–1987, embracing an area larger than 2.5 million km^2. For the 24-month duration, the most intensive drought event occurred in the early 1980s (1982–1984), affecting an area of less than 0.5 million km^2 in the north of the Southwest river basins.

6 Possible reasons for the regional shift in drought events

The annual average precipitation amounts per decade over the ten large river basins during the 1960s, 1970s, 1980s, 1990s, 2000s and 2011–2013 are presented in Fig. 13. Except for the persistent increase in precipitation in the Northwest river basins and decrease in the Haihe River basin for the period 1961–2010, the decadal differences in precipitation in the other river basins imply a rather natural variability. The 2000s is the decade with the lowest precipitation amounts in all north-central river basins (Songhuajiang, Liaohe, Haihe, Yellow River, and Yangtze River), while the period 2011–2013 shows a sharp increase in precipitation for most of these basins, resulting in significant trends toward wetness in these north-central river basins for the early twenty-first century, which strongly supports the findings in the SPI for these river basins. Furthermore, the lower precipitation amounts have been observed in the Yangtze River basin and the Southwest river basins, leading to the ‘stable’ dryness trend and experienced drought events in Southwest China. Our findings are in line with

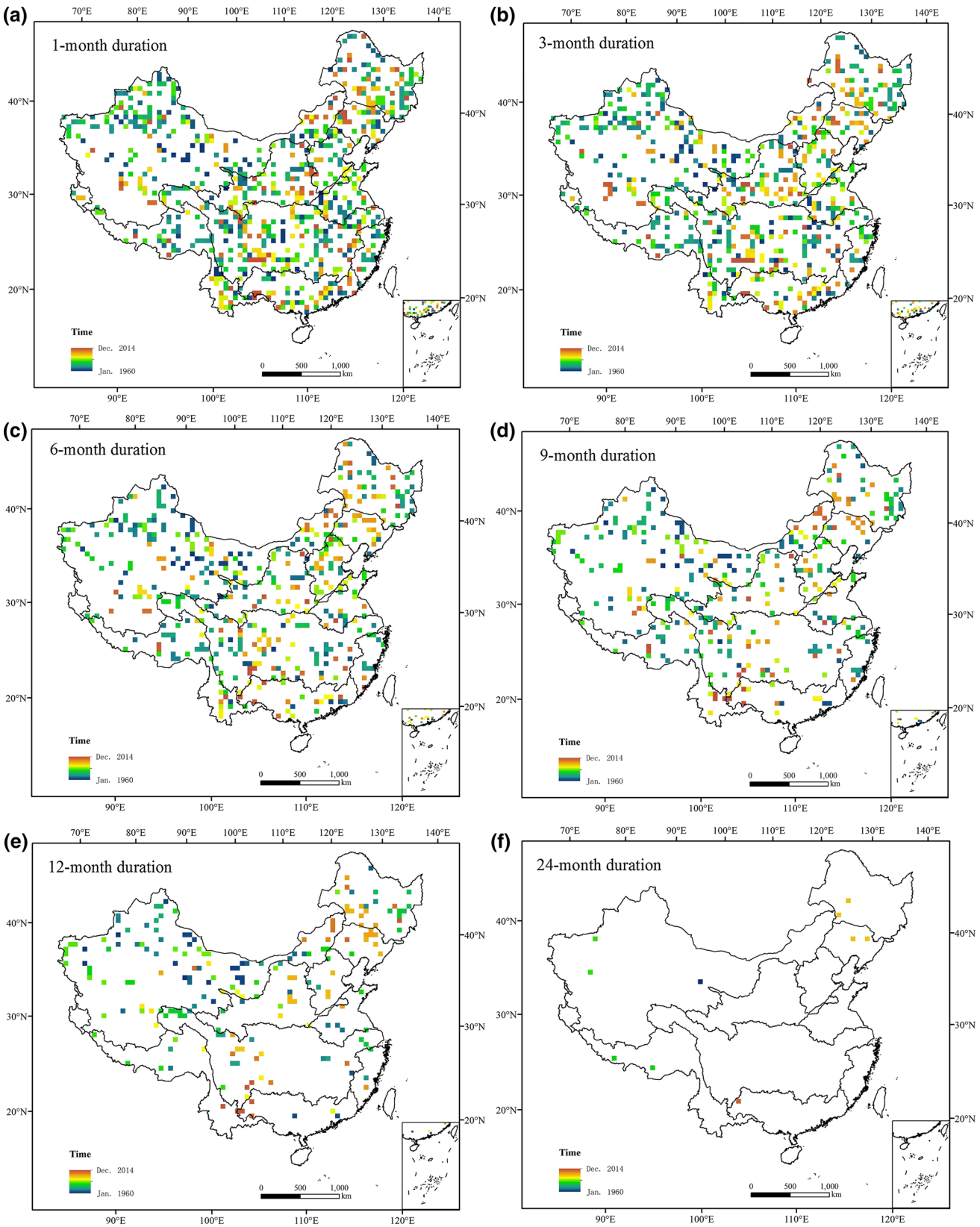

Fig. 9 Spatial distribution of drought centers of all droughts with a contiguous area above 50,000 km^2 for different durations (1-, 3-, 6-, 9-, 12-, 24-months) in China for 1960–2013

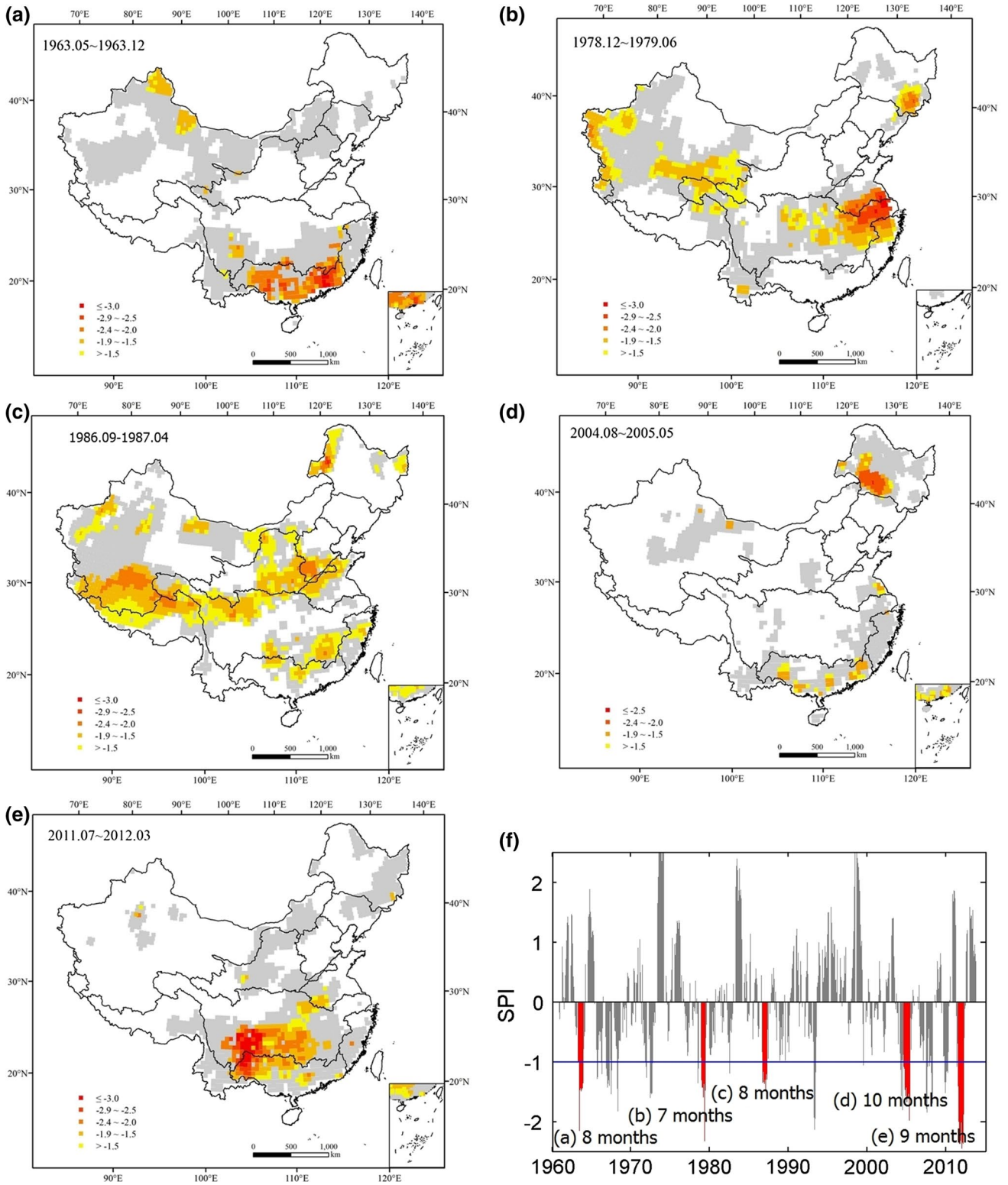

Fig. 10 Spatial distributions of droughts in five selected dryness period (**a**–**e**). *Gray shadings* represent the extent of droughts without considering the duration; *Colored shadings* indicate the drought area and intensity for the duration covering the whole selected period; the *red shaded bars* in **f** represent the five major drought period

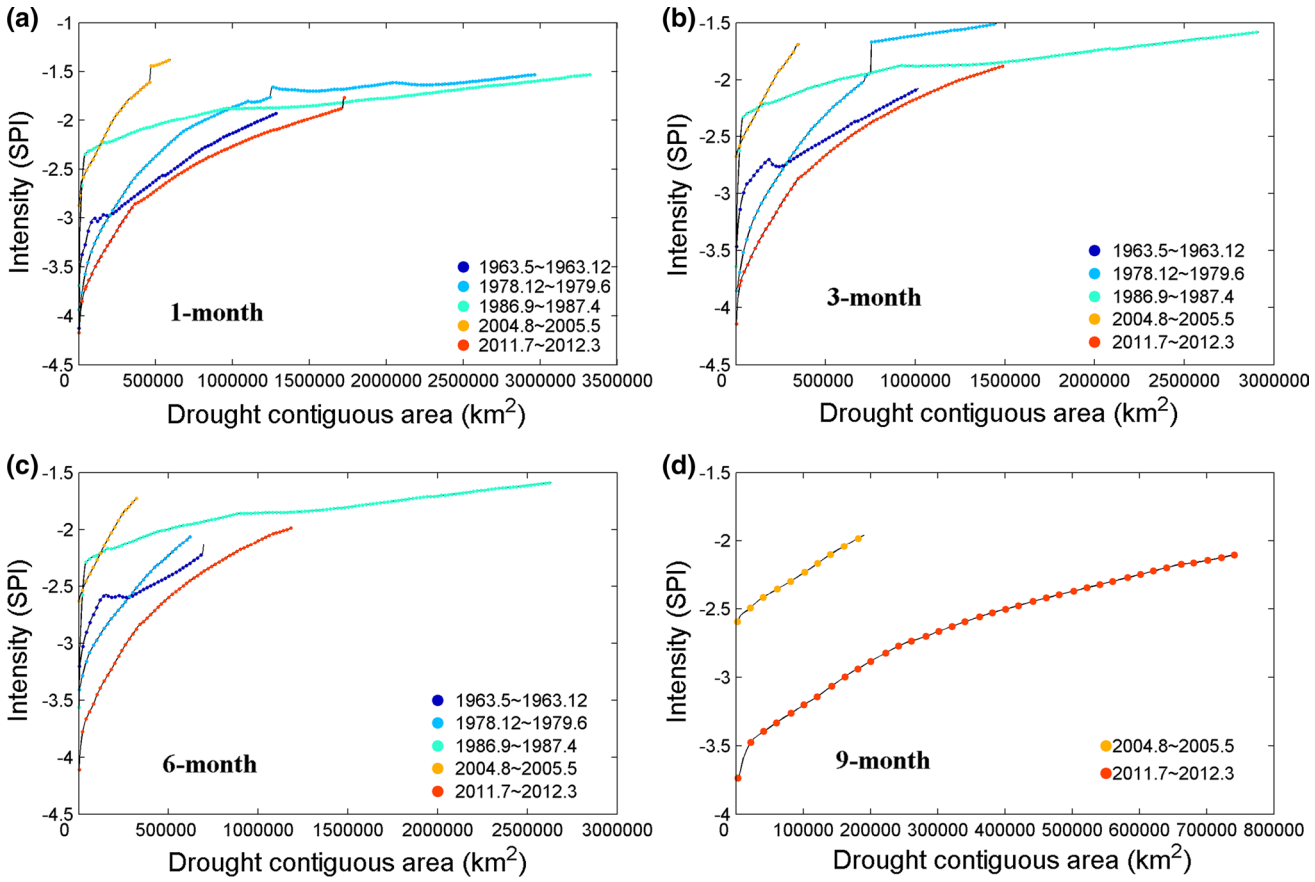

Fig. 11 Intensity–area–duration (IAD) curves for the five major drought events with a 1-, 3-, 6-, and 9-months duration; *Different colors* denote the five major drought events and their specific start and end time as identified for China during the period 1960–2013

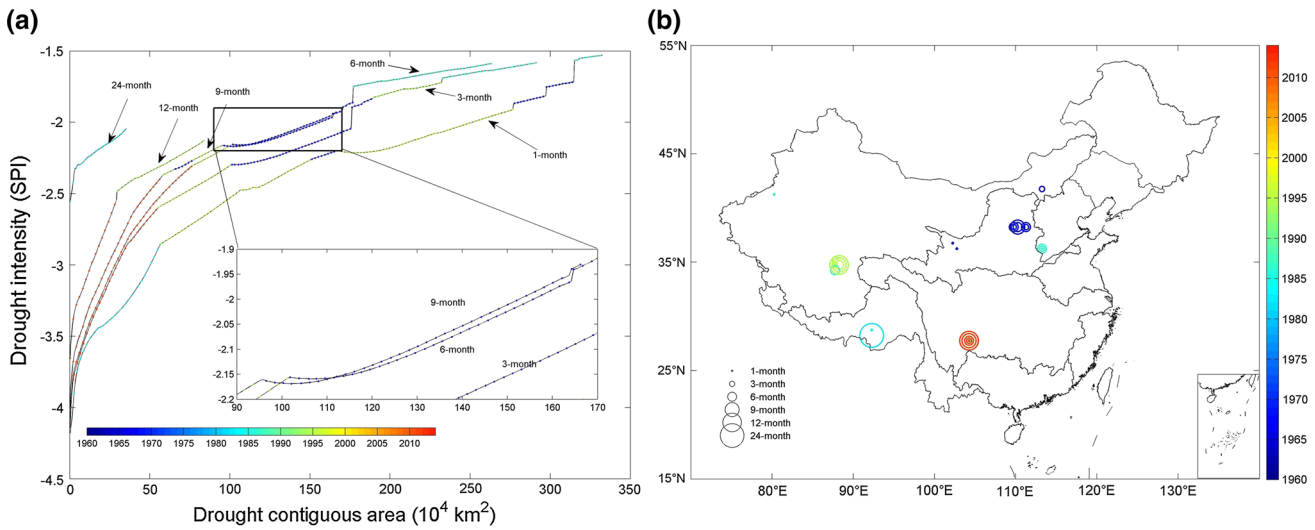

Fig. 12 IAD envelope curves (**a**) and their drought center (**b**) for six predefined durations (i.e. drought durations of 1-, 3-, 6-, 9-, 12-, 24-months); *Different colors* denote the specific start time as identified for China during the period 1960–2013

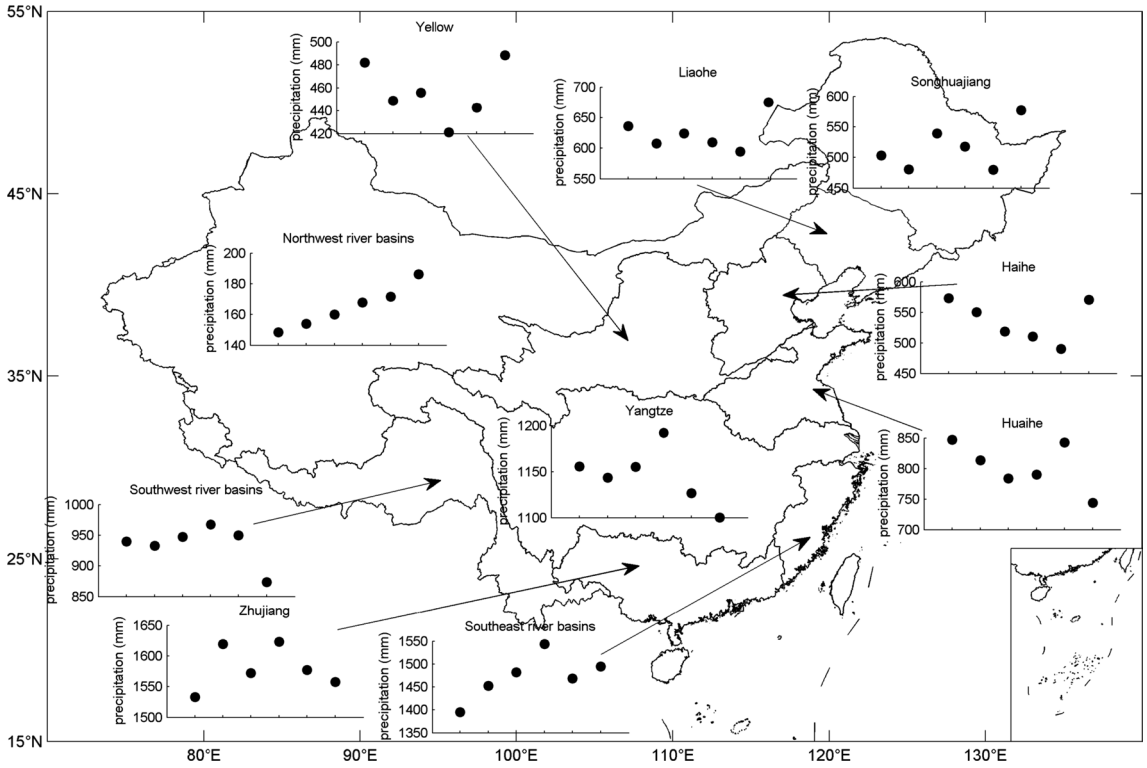

Fig. 13 Average annual precipitation amounts per decade of ten major hydrological regions of China for 1960–2013

the findings of Chen and Sun (2015), who found relatively large responses of droughts to precipitation in southern China, but only small responses in northern China. The regional shifts in drought events can also be related to the varying changes in precipitation extremes over various regions of China in the last decades (Zhao et al. 2012; Fischer et al. 2012).

Furthermore, the precipitation patterns are connected with the atmosphere–ocean interaction (Saji et al. 1999; Wu and Kirtman 2007). The summer precipitation in China is highly correlated with the 500 hpa geopotential height. This circulation feature, the subtropical Western Pacific high, is the key aspect of the Asian monsoon (Huang and Yan 1999; Gong and Ho 2002). The subtropical high is strongly related with the Tropical East Pacific sea surface temperature (SST), which leads by one or two seasons to the SST of the Tropical Indian Ocean (Gong and Ho 2002). The southward shift in the subtropical Western Pacific high is caused by an increase in both, the spring SST of the Tropical East Pacific and the summer SST of the Tropical Indian Ocean. These decadal increases brought more summer precipitation to the south of China, but less precipitation to the north of China (Gong and Ho 2002; Yang and Lau 2004). Furthermore, the Eastern Pacific El Niño phenomenon (warm SST anomaly above normal in 150°–90°W, 5°S–5°N) is associated with the increase in autumn precipitation over southern China, while La Niña events and the Central Pacific El Niño (160°E–150°W, 5°S–5°N) are associated with deficits in autumn precipitation (Zhang et al. 2014). Since the 1990s, no significant changes in the zonal location of La Nina events as well as in the occurrence of the Eastern Pacific El Niño are found, while more frequent occurrences of the Central Pacific El Nino with an increasing intensity have been observed (Kug et al. 2009; Lee and McPhaden 2011; Zhang et al. 2014). Due to the changes in El Niño pattern in recent years, strong anomalous cyclones developed in the Northwest Pacific and lead to the reduction in autumn precipitation over Southwest China (Zhang et al. 2013b), which is most likely the major reason for the observed drought in Southwest China in 2009–2010. For the Northwest river basins of China, more moisture in the mid-latitude atmosphere has been transported from the maritime east to the northwest (Tao et al. 2014). For the period 2000–2013, although a persistent increase in the Tropical Indian Ocean SST is found, the tropical East Pacific SST (main factor) decreased in all seasons (Fig. 14d, f). The subtropical Western Pacific high is more likely to shift northward. As seen in Fig. 14c, the subtropical high, influenced by the Tropical East Pacific and Tropical Indian Ocean, moved southwest before the twenty-first century and then shifted northeast. These changes have contributed to the dryness trend in Southwest

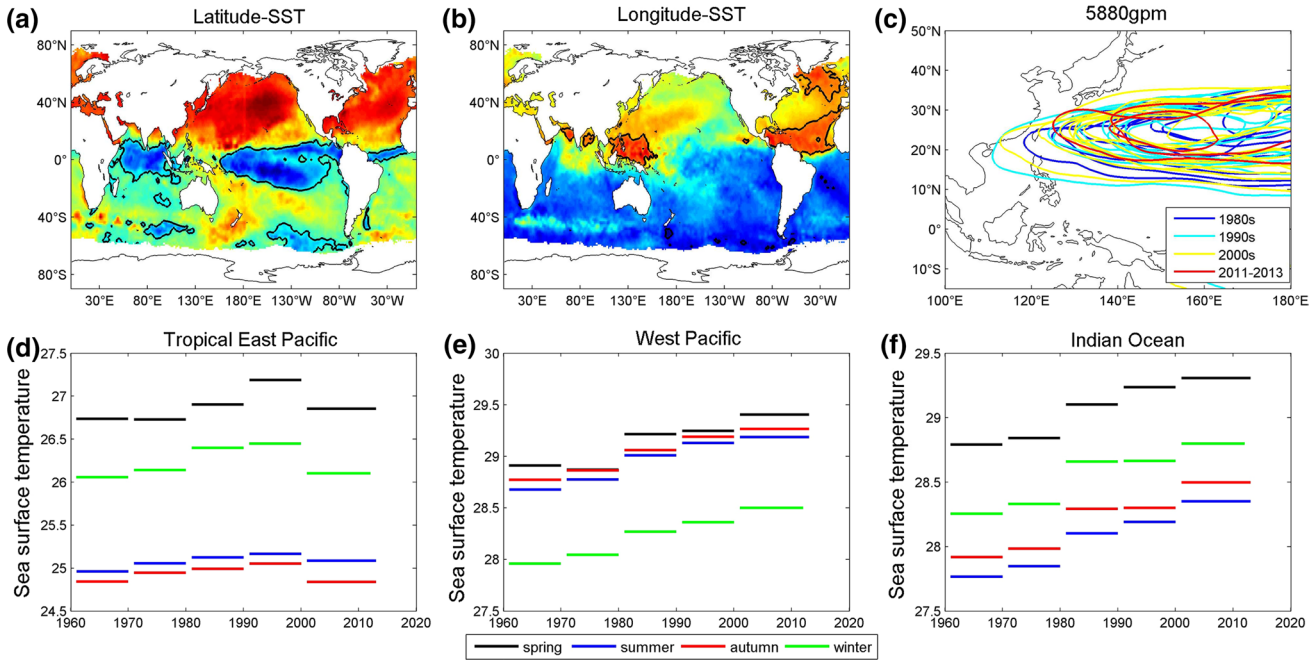

Fig. 14 Relationship between sea surface temperature and annual average **a** latitude and **b** longitude of drought centers, the *bold line* indicates significance at the 95 % confidence level; **c** *contour lines* for 5880 gpm at 500 hpa geopotential height for average location of the subtropical Western Pacific high during summer per decade; and **d–f** decadal average sea surface temperature in the Tropical East Pacific (150°W–90°W, 5°S–5°N), the Tropical Indian Ocean (60°E–100°E, 10°S–10°N), and the West Pacific (120°E–150°E, 4°S–15°N); the SST data has been derived from the Met Office Hadley Centre observations datasets, and the ERA-interim geopotential height data has been provided by the European Centre for Medium Range Weather Forecast

China and the wetness trend in North China during 2000–2013. The further decrease in SST of the Tropical East Pacific and the northward shift of the subtropical Western Pacific high in 2011–2013 may cause more intense drought events in Southwest China, which is in line with the experienced drought events in 2011–2012 detected by the IAD method.

7 Conclusions and discussion

Based on monthly precipitation datasets, the SPI for various hydrological regions are calculated and analyzed on its trends and tendencies to dry conditions over China for the period 1960–2013. Furthermore, the intensity and spatio-temporal drought characteristics are analyzed by applying the IAD method on regional SPI values and by including the visualization of corresponding curves and maps.

Based on the detected trends for the period 1960–2013, a regional band of significant increases in droughts can be distinguished reaching from the southwest to the northeast of China (with most of the stations showing significances at the 95 % confidence level). Additionally, significant trends toward more wet conditions are found in the western parts of China. These findings are in line with the results by Zhai et al. (2010), who analyzed the SPI for whole China for the period 1961–2005. In addition, for recent years (2000–2013), most of the ten major hydrological regions in China show opposite trends in the SPI when compared to the whole study period (1960–2013) except for the central and southwestern parts of China. The "stable" trend to dry conditions in the central and southwestern parts for both periods can be linked to the most recent severe drought events occurring in these regions, e.g. extreme drought events of 2009/2010 over southwestern China (Yang et al. 2012b). Additionally, the western and northeastern river basins experienced stronger magnitudes in the SPI in the early twenty-first century supporting the assumption of intensification due to global warming. The other river basins experienced rather stable magnitudes implying a typical oscillation without notable influences by global warming but rather natural climate variability.

Drought events with short duration occur more frequently in humid regions, while drought events with longer duration are more common in the arid and semi-arid regions in China. Except for the Haihe River basin and the middle and lower Yellow River basin, the intensity and duration of drought events shows an increasing tendency to stronger and longer droughts during the period 1960–2013. For the study period, a decrease in the average and the maximum contiguous areas (larger than 50,000 km^2) for different durations (1, 3, 6, 9, and 12 months)

has been found. The decreasing trend is also identified by two vegetation indexes, which show a decreasing trend for the period 1982–2005 over China (Li et al. 2013). This indicates that the more recent drought events affected a smaller area than in the mid-twentieth century. Accordingly, a spatial–temporal shift from short-term but large-sized droughts to more severe and long-term but small-sized drought events has been detected in China for the period 1960–2013. A regional shift of the centers of the average and maximum contiguous drought events occurred from the northwest to the southeast within Central China. While in the mid-twentieth century most severe drought events occurred in the arid and semi-arid regions in Northern and Western China, in the early twenty-first century most intensive droughts affected the central and southern areas of China. By using a standardized precipitation evapotranspiration index over China, Chen and Sun (2015) detected that droughts occurred more frequent and were more severe in the early twenty-first century, which supports our findings for the northern basins, but cannot be agreed on for the southern river basins. He et al. (2011) detected that the spatial extents of droughts in the eastern parts of China are more severe than in the western parts for the period 1960–2008, which is to some extent in line to our findings in the trends and spatial distribution of drought characteristics in China. In our study, a regional shift of drought centers is identified by analyzing the decadal latitudinal and longitudinal location averages. It was found that the latitudinal variation in drought events is strongly correlated with the subtropical high, which is influenced by higher sea surface temperatures of the tropical West Pacific and tropical Indian Ocean. Additionally, the longitudinal variation in drought events is highly correlated with the wetness in western China, which shows correlations to the SST in the West Pacific, the North Atlantic, and the Arabian Sea.

The five major drought periods over whole China occurred in 1963, 1978/1979, 1986/1987, 2004/2005, and 2011/2012. When various drought durations are considered, several regional characteristics in intensity and areal extent can be distinguished. Detailed IAD curves have been generated and analyzed for the five major drought periods. The most recent droughts in the early-twenty-first century are the most severe droughts covering relatively small areas (below 0.7 million km^2) in the Southwest of China for their entire durations. As described by Tang et al. (2014), two heavy droughts in 2009–2010 and 2011–2012 were detected in Southwestern China with the latter being the most severe in the early-twenty-first century. While the IAD compare the drought events in the five major drought periods as interpreted for whole China, the IAD envelope curves identified the most severe drought events at each contiguous area affected by drought in the whole study period. Here, two severe drought events (1986–1987, 2011–2012) are equally found among the five major drought periods, when either intensity or contiguous area is considered. By focusing on the area, three additional drought periods (1965–1966, 1982–1984, 1994–1995) are found to rank higher. The drought event in 1965–1966 in the North of China is one of the three exceptional drought events for the period 1500–2000 in terms of drought intensity, duration and spatial coverage as described by Shen et al. (2007). The droughts in 1982–1984 located in the western part of China lasted 24 months. In 1994–1995, the drought with the highest intensity for the duration from 1- to 3-month covered a contiguous area larger than 2 million km^2 and was located in the far west of China. Although the longer duration in 1982–1984 and larger drought area in 1994–1995, these droughts probably did not have so much adverse impacts on the population, agriculture and other sectors as the other major droughts, due to their occurrence in the least populated area of China.

In future, higher drought risks are projected based on a CMIP5 (Coupled Model Intercomparison Project phase 5) model ensemble under different RCPs (Representative Concentration Pathways) for Southwest and East China in the twenty-first century (Wang and Chen 2014; Yin et al. 2015). The average drought centers shifted from the northwest to the central part of China in the last 54 years. Based on the above findings and considering the decreasing trend in the average contiguous area (larger than 50,000 km^2), the location of the average drought center could move further towards the southeast of China. Such possible changes in the average location of drought centers will be investigated by applying a regional climate model in following study paper.

Acknowledgments This study was supported by the National Basic Research Program of China (973Program; Nos. 2012CB955903, 2013CB430205) and the National Natural Science Foundation in China (No. 41571494). The authors also thank the National 1000 Talent program (Y474171) for supporting this work.

References

Andreadis KM, Clark EA, Wood AW et al (2005) Twentieth-century drought in the conterminous United States. J Hydrometeorol 6:985–1001

Biondi F, Kozubowski TJ, Panorska AK et al (2008) A new stochastic model of episode peak and duration for eco-hydro-climatic applications. Ecol Model 211:383–395

Bordi I, Fraedrich K, Petitta M et al (2005) Large-scale analysis of drought in Europe using Ncep/Ncar and Era-40 Re-analysis data sets. Eur Water 9(10):35–42

Chen HP, Sun JQ (2015) Changes in drought characteristics over China using the Standardized Precipitation Evapotranspiration Index. J Clim 28:5430–5447

Field CB, Barros V, Stocker TF, IPCC et al (2012) Managing the risks of extreme events and disasters to advance climate change adaptation. Cambridge University Press, New York, p 582

Fischer T, Gemmer M, Liu L, Su BD (2011) Temperature and precipitation trends and dryness/wetness pattern in the Zhujiang River Basin, South China, 1961–2007. Quatern Int 244(2):138–148

Fischer T, Gemmer M, Liu LL, Su BD (2012) Change-points in climate extremes in the Zhujiang River Basin, South China, 1961–2007. Clim Change 110(3–4):783–799

Gemmer M, Becker S, Jiang T (2004) Observed monthly precipitation trends in China 1951–2002. Theoret Appl Climatol 77:39–45

Gong DY, Ho CH (2002) Shift in the summer rainfall over the Yangtze River valley in the late 1970s. Geophys Res Lett. doi:10.1029/2001GL014523

Hansen J, Ruedy R, Sato M, et al (2010) Global surface temperature change. Rev Geophys 48:RG4004

He B, LüA F, Wu JJ et al (2011) Drought hazard assessment and spatial characteristics analysis in China. J Geog Sci 21(2):235–249

Huang G, Yan ZW (1999) The east Asia summer monsoon circulation anomaly index and its interannual variations. Chin Sci Bull 44:1325–1329

Kamali B, Abbaspour KC, Lehmann A et al (2015) Identification of spatiotemporal patterns of biophysical droughts in semi-arid region: a case study of the Karkheh river basin in Iran. Hydrol Earth Syst Sci 12:5187–5217

Kug JS, Jin FF, An SI (2009) Two types of El Niño events: cold tongue El Niño and warm Pool El Niño. J Clim 22:1499–1515

Kyoung M, Kwak J, Kim D et al (2011) Drought analysis based on SPI and SAD curve for the Korean peninsula considering climate change. In: Blanco J (ed) Climate change: geophysical foundations and ecological effects. InTech, Croatia, pp 195–214

Lawrimore JH, Menne MJ, Gleason BE et al (2011) An overview of the Global Historical Climatology Network monthly mean temperature data set, version 3. J Geophys Res Atmos. doi:10.1029/2011jd016187

Lee T, McPhaden MJ (2011) Increasing intensity of El Niño in the central-equatorial Pacific. Geophys Res Lett 37:L14603. doi:10.1029/2010GL044007

Li B, Su HB, Chen F et al (2013) The changing characteristics of drought in China from 1982 to 2005. Nat Hazards 68:723–743

McKee TB, Doesken NJ, Kleist J (1993) The relationship of drought frequency and duration to time scales. Preprints. In: Eighth conference on applied climatology, Anaheim, CA, Amer. Meteor. Soc., pp 179–184

Mishra AK, Singh VP (2010) A review of drought concepts. J Hydrol 391:202–216

Narasimhan B, Srinivasan R (2005) Development and evaluation of Soil Moisture Deficit Index (SMDI) and Evapotranspiration Deficit Index (ETDI) for agricultural drought monitoring. Agric For Meteorol 133(1–4):69–88

Qian WH, Shan XH, Zhu YF (2011) Ranking regional drought events in China for 1960–2009. Adv Atmos Sci 28(2):310–321

Qin DH, Zhang JY, Shan CC et al (2015) China national assessment report on risk management and adaptation of climate extremes and disasters. Science Press, China

Rohde R, Muller RA, Jacobsen R et al (2013) A new estimate of average earth surface land temperature spanning 1753 to 2011. Geoinfor Geostat Overv 1:1

Saji NH, Goswami BN, Vinayachandran PN et al (1999) A dipole model in the tropical Indian Ocean. Nature 401:360–363

Samaniego L, Kumar R, Zink M (2013) Implications of Parameter uncertainty on soil moisture drought analysis in Germany. J Hydrometeorol 14:47–68

Sheffield J, Wood EF (2007) Characteristics of global and regional drought, 1950–2000: analysis of soil moisture data from off-line simulation of the terrestrial hydrologic cycle. J Geophys Res 112:D17115

Sheffield J, Andreadis KM, Wood EF et al (2009) Global and continental drought in the second half of the twentieth century: severity–area–duration analysis and temporal variability of large-scale events. J Clim 22(8):1962–1981

Shen C, Wang WC, Hao Z et al (2007) Exceptional drought events over eastern China during the last five centuries. Clim Change 85:453–471

Shi YF, Shen YP, Li DL et al (2003) Discussion on the present climate change from warm-dry to warm-wet in Northwest China. Quat Sci 23:152–164

Smerdon JE, Seager R, Cook ER (2014) Pan-continent droughts in North America over the last millennium. J Clim 27:383–397

Tang JS, Cheng HW, Liu L (2014) Assessing the recent droughts in Southwestern China using satellite gravimetry. Water Resour Res 50(4):3030–3038

Tao H, Gemmer M, Bai YG et al (2011) Trends of streamflow in the Tarim River Basin during the past 50 years: human impact or climate change? J Hydrol 400:1–9

Tao H, Borth H, Fraedrich K et al (2014) Drought and wetness variability in the Tarim River Basin and connection to large-scale atmospheric circulation. Int J Climatol 34(8):2678–2684

Vicente-Serrano SM, Begueria S, Lorenzo-Lacruz J et al (2012) Performance of drought indices for ecological, agricultural, and hydrological applications. Earth Interact 16(10):1–27

Wang L, Chen W (2014) A CMIP5 multimodel projection of future temperature, precipitation, and climatological drought in China. Int J Climatol 34:2059–2078

World Meteorological Organization (WMO) (2012) Standardized Precipitation Index User Guide (WMO-No.1090), Geneva

Wu R, Kirtman BP (2007) Regimes of seasonal air–sea interaction and implications for performance of forced simulations. Clim Dyn 29:393–410

Wu H, Hayes MJ, Wilhite DA et al (2005) The effect of the length of record on the standardized precipitation index calculation. Int J Climatol 25:505–520

Xu K, Yang DW, Yang HB et al (2015) Spatio-temporal variation of drought in China during 1961–2012: a climatic perspective. J Hydrol 526:253–264

Yang F, Lau KM (2004) Trend and variability of China precipitation in spring and summer: linkage to sea-surface temperature. Int J Climatol 24:1625–1644

Yang CG, Yu ZB, Hao ZC et al (2012a) Impact of climate change on flood and drought events in Huaihe River Basin, China. Hydrol Res 43(1–2):14–22

Yang J, Gong DY, Wang WS et al (2012b) Extreme drought event of 2009/2010 over southwestern China. Meteorol Atmos Phys 115:173–184

Yin Y, Ma D, Wu S et al (2015) Projections of aridity and its regional variability over China in the mid-twenty-first century. Int J Climatol. doi:10.1002/joc.4295

Yu XY, He XY, Zheng HF et al (2014) Spatial and temporal analysis of drought risk during the crop-growing season over northeast China. Nat Hazards 71(1):275–289

Zhai JQ, Su BD, Krysanova V et al (2010) Spatial variation and trends in PDSI and SPI indices and their relation to streamflow in 10 large regions of China. J Clim 23:649–663

Zhai JQ, Gao B, Zhu XY (2014) Fact sheet on climate disasters in China. In: Wang GW, Zheng GG (eds) Annual report on actions to address climate change. Social Sciences Academic Press, China

Zhang MJ, He JY, Wang BL et al (2013a) Extreme drought changes in South west China from 1960-2009. J Geog Sci 23(1):3–16

Zhang WJ, Jin FF, Zhao JX et al (2013b) The possible influence of a nonconventional El Niño on the severe autumn drought of 2009 in Southwest China. J Clim 26:8392–8405

Zhang WJ, Jin FF, Turner A (2014) Increasing autumn drought over southern China associated with ENSO regime shift. Geophys Res Lett 41:4020–4026

Zhao GJ, Mu XM, Hörmann G et al (2012) Spatial patterns and temporal variability of dryness/wetness in the Yangtze River Basin, China. Quatern Int 282:5–13